

1 Early warning of MIB episode based on gene abundance and
2 expression in drinking water reservoirs

3 Tengxin Cao^{a,f,g}, Jiao Fang^a, Zeyu Jia^{c,a}, Yiping Zhu^d, Ming Su^{a,b,g,*}, Qi Zhang^e, Yichao Song^d,
4 Jianwei Yu^{a,b,g}, Min Yang^{b,a,g,*}

^aKey Laboratory of Drinking Water Science and Technology, Research Center for Eco-Environmental Sciences, Chinese Academy of Sciences, P.O. Box 2871, Beijing, 100085,

^bNational Engineering Research Center of Industrial Wastewater Detoxication and Resource Recovery, Research Center for Eco-Environmental Sciences, Chinese Academy of Sciences, P.O. Box 2871, Beijing, 100085,

^cYangtze Eco-Environment Engineering Research Center, China Three Gorges Corporation, Beijing, 100038,

^dShanghai Chengtou Raw Water Co. Ltd., Beiai Rd. 1540, Shanghai, 200125,

^eInstitute of Hydrobiology, Chinese Academy of Sciences, No. 7 Donghu South Road, Wuchang, Wuhan, 430072,

^fSino-Danish College, University of Chinese Academy of Sciences, Beijing, 100049,

^gUniversity of Chinese Academy of Sciences, Beijing, 100049,

5 **Abstract**

Cellular 2-methylisoborneol (MIB) yield of cyanobacteria varies under different conditions according to culture studies and field investigations, the causal mechanism remains unclear and results in ineffective MIB prediction. Through an intensive field survey during an MIB episode produced by *Pseudanabaena cinerea* in QCS reservoir, we demonstrated that MIB synthesis (*mic*) gene abundance (DNA) and expression (RNA) might be useful as parameters for early warning of MIB production. It was found that the abundance of *mic* DNA and RNA peaked ahead of MIB concentrations by 10 and 7 days, respectively. In addition, the RNA abundance ($R^2 = 0.45$, $p < 0.01$) showed a slightly higher correlation with MIB compared to DNA abundance ($R^2 = 0.37$, $p < 0.01$), suggesting that the conditions for the growth of *Pseudanabaena cinerea* might be slightly different from those for *mic* gene expression, which was verified by a culture experiment. The highest cell growth was obtained under $36 \mu\text{mol photons m}^{-2} \text{s}^{-1}$, while the highest cellular MIB yield and *mic* gene expression level were obtained under $85 \mu\text{mol photons m}^{-2} \text{s}^{-1}$. Our results clearly supported that light intensity was the virtual regulator governing the *mic* gene expression within the controlled culture experiment and the actual MIB episode in the reservoir. Besides

these results, we developed an early warning model using *mic* gene abundance as an indicator of MIB episodes, which was verified in two other reservoirs. Our findings highlight the effect of light intensity on *mic* gene expression and MIB synthesis and provide an early warning tool targeting MIB episode prediction, which therefore should be of importance for source water authorities.

6 *Keywords:* 2-methylisoborneol (MIB), MIB synthesis gene, *Pseudanabaena*, Prediction, Light
7 intensity, Gene expression, Reservoir

8 **1. Introduction**

9 Taste and odor issues, particularly the musty odor caused by 2-methylisoborneol (MIB), have
10 become a major challenge for water quality (Izaguirre and Taylor, 2007; Lanciotti et al., 2003;
11 Yang et al., 2008; Sun et al., 2013). If the MIB concentration in source water is over 400 ng L⁻¹, for
12 example, dosing with powdered activated carbon alone may not be enough to achieve the goal
13 of <10 ng L⁻¹ (odor threshold concentration) in purified water (Cook et al., 2001; Zamyadi et al.,
14 2015). Although MIB was first identified as the volatile secondary metabolite produced by acti-
15 nomycetes (Gerber, 1979), filamentous cyanobacteria including *Pseudanabaena*, *Planktothrix*,
16 *Phormidium*, *Oscillatoria*, *Lyngbya*, *Planktothricoides*, etc. are the major producers of MIB in
17 drinking water sources (Persson, 1996; Watson et al., 2008, 2016; Su et al., 2015; Lu et al., 2022).
18 MIB concentration in actual water is governed by the growth of MIB producer(s), the expres-
19 sion level of MIB synthesis gene and hydrological transportation of MIB diffusion. Water tem-
20 perature, nutrients, light availability, and hydrodynamics have been revealed as the driving fac-
21 tors affecting the growth of MIB producers based on field investigation and culture experiments
22 (Kakimoto et al., 2014; Jia et al., 2019; Wang and Li, 2015). In comparison with scum-forming
23 cyanobacteria, the growth of which is mainly driven by nutrient availability, the driving forces
24 for the growth of MIB producers are quite complicated. Because of their relatively large cellular
25 sizes, these filamentous cyanobacteria have a strong capacity to harness light energy (Halstvedt

*Corresponding author

Email addresses: mingsu@rcees.ac.cn (Ming Su), yangmin@rcees.ac.cn (Min Yang)

26 [et al., 2007](#); [Su et al., 2014](#)), which allows them to live in low-light conditions ([Su et al., 2019](#)).
27 Such a feature, however, makes them susceptible to competition from other cyanobacteria, leav-
28 ing a narrow niche for themselves in natural reservoirs/lakes ([Su et al., 2019](#)). Accordingly, MIB
29 producers are usually not the dominant cyanobacteria species in a particular water system, and
30 their occurrence and MIB episodes only last for normally no longer than 2 months ([Izaguirre
31 and Taylor, 2007](#); [Su et al., 2015, 2021](#); [Wu et al., 2021](#)). Nevertheless, cellular MIB yields still
32 show great variation during that period, even when the water temperature and nutrient con-
33 ditions are rather stable ([Chiu et al., 2016](#); [Huang et al., 2018](#)), suggesting that the ambient
34 environmental factors not only govern the growth of MIB producers, but also affect cellular MIB
35 productivity. Furthermore, MIB is synthesized through the isoprenoid pathway, and shares a
36 common precursor geranyl pyrophosphate (GPP) with photosynthesis pigments chlorophyll *a*
37 (chl *a*), Carotenoids, and Xanthophylls in cyanobacteria ([Zimba et al., 1999](#)), suggesting that MIB
38 production is a light-dependent process. In addition to solar irradiance, light availability is also
39 governed by the water extinction coefficient and mixing depth. Therefore, we speculate that
40 underwater light availability could possibly be an important driving factor for the growth of MIB
41 producers as well as MIB biosynthesis in natural water bodies, which makes the MIB episodes
42 quite unpredictable based on traditional methods ([Chiu et al., 2016](#); [Huang et al., 2018](#)). This
43 has created a difficult situation for waterworks trying to adjust their treatment processes.

44 Quantification of functional genes has been regarded as a potential method for cyanobacte-
45 rial metabolite prediction, e.g., the toxin-encoding genes have been used to predict microcystin
46 production by as much as 7 days in advance ([Lu et al., 2020](#)). The pathway of MIB biosynthesis
47 is nearly the same in cyanobacteria ([Giglio et al., 2011](#); [Wang et al., 2011](#)) and actinomycetes
48 ([Komatsu et al., 2008](#)). It consists of two main steps from the precursor geranyl diphosphate
49 (GPP), including 1) a methylation process from GPP to methyl-GPP catalyzed by methyltrans-
50 ferase (GPPMT), and 2) a cyclization process from methyl-GPP to MIB by MIB synthase (MIBS).
51 These two processes do not fully match with cyanobacteria taxonomy, so cell morphology-based
52 cyanobacteria identification is therefore unable to distinguish the MIB producers making it dif-
53 ficult to evaluate the MIB production in drinking water reservoirs/lakes. Thus, the abundance

54 of genes associated with GPPMT/MIBS and their expression have merit as fundamental indica-
55 tors for MIB episodes, as verified in field studies (Chiu et al., 2016; Kim et al., 2020; Lu et al.,
56 2019; Rong et al., 2018; Wang and Li, 2015). In view of the fact that the sequences of the two
57 genes vary somewhat among strains, we have developed a pair of universal primers (MIBQSF/R)
58 targeting the MIBS gene (*mic* gene) of all known MIB-producing strains, and validated it to be
59 MIB-specific based upon samples from 9 reservoirs and 17 cultured strains (Suruzzaman et al.,
60 2022). In addition to the presence of the gene in the genome, the expression of the *mic* gene
61 is also essential to the biosynthesis of MIB. Therefore, it may be possible to use *mic* gene abun-
62 dance and expression to predict the occurrence and strength of MIB episodes.

63 On the basis of the description from above literatures and our previous studies, we proposed
64 the hypothesis that light intensity is a more important regulator of MIB synthesis gene expres-
65 sion compared to water temperature and nutrient concentrations for an actual MIB episode. A
66 systematic field investigation was performed in Qingcaosha (QCS) Reservoir including the spatial
67 and temporal distributions of MIB, MIB producers and *mic* gene abundance/expression. At the
68 same time, the effect of light intensity on the cell growth, MIB production, cellular MIB yield
69 and *mic* gene expression of the MIB-producing *Pseudanabaena* strain (*Pseudanabaena cinerea*
70 FACHB 1277) were determined through culture experiments. Finally, valid early warning indica-
71 tors targeted for MIB prediction were proposed and applied to drinking water reservoirs.

72 **2. Methods and Materials**

73 *2.1. Study area and sampling sites*

74 QCS Reservoir (32°27'N, 121°38'E, Fig. S1, Fig. S2), located in the estuary of the Yangtze River,
75 is the major source of drinking water for Shanghai (Su et al., 2021), and has suffered from MIB
76 problems for several years. The reservoir has the maximum storage capacity of 437.5 GL and
77 the surface area of 66.15 km². According to the temperature profile observed in our previous
78 study, the water bodies showed the well vertical mixed characteristics year-round. A total of 19
79 sampling sites were selected from Upstream river water (1 site), North branch (3 sites), South

80 branch (4 sites), and Middle section (11 sites) to investigate the spatial distribution of MIB con-
81 centrations in 2021 (Fig. S1, Table S1) according to bathymetry (Fig. S2). According to the tem-
82 perature profile observed in our previous study (Su et al., 2021), the water bodies showed the
83 well vertical mixed characteristics year-round. Since this reservoir is well-mixed, 5 L water sam-
84 ples from the surface layer (0.5 m) of all sites were collected by Kemmerer water sampler weekly
85 for physico-chemical measurement, algal enumeration, and molecular detection during an MIB
86 episode. Meanwhile, daily sampling was conducted in QC10 (located in the North branch, Fig.
87 S1) to follow the temporal dynamics of MIB and related gene abundances. All samples were
88 stored at 4 °C within 24 h until use.

89 MIB concentrations were determined using solid-phase micro-extraction (SPME) coupled with
90 gas chromatography-mass spectrometry (GC-MS) (Su et al., 2015). The physico-chemical prop-
91 erties including water temperature, dissolved oxygen (DO), pH, and turbidity were measured
92 using a multiple-probe instrument (EXO2, Xylem, USA) *in-situ*. Water transparency, expressed
93 as secchi depth (SD), was measured by a Secchi disk (diameter: 20 cm, black and white). Total
94 phosphorus (TP), total nitrogen (TN), nitrate nitrogen (NO₃-N) and ammonia nitrogen (NH₄-N)
95 were measured according to the national water quality standards of China. Air temperature and
96 solar irradiance were obtained from the China Meteorological Data Service Center (CMDC). The
97 water level and inlet/outlet volume were obtained from the reservoir authority. Hydraulic reten-
98 tion time (HRT) was determined based on inlet/outlet volume and reservoir storage. The 100
99 mL subsamples for phytoplankton cell counting were preserved with 5 % Lugol's iodine and con-
100 centrated to 10 mL after sedimentation for 48 h. Cell counting was performed using a counting
101 chamber (S52, 1 mL, Sedgewick-Rafter) under a microscope (OLYMPUS BX51, Olympus Optical,
102 Tokyo, Japan), and the cyanobacterial species was identified according to (Komarek et al., 2014).
103 The filamentous cyanobacteria abundances were quantified based on the length of each fila-
104 ment and the mean cell length of each strain, and the number of cells in colony species such
105 as *Microcystis* sp. was estimated based on colony volume and mean cell density. The mean
106 cell morphological characteristics including cell length, cell volume etc. were determined ac-
107 cording to more than 50 filaments/colonies of each strain using a self-developed cell-counting

108 tool (CCT v1.4, <https://drwater.rcees.ac.cn>, in Chinese); more details can be found in Su et al.
109 (2015). Jinze (JZ) Reservoir (31°03'N, 120°95'E) and Lianghai (LH) Reservoir (29°98'N, 121°16'E)
110 were selected to validate the *mic* gene-based early warning method, and the samples collection,
111 storage, and analysis methods were the same as those of QCS Reservoir.

112 2.2. DNA and RNA extraction

113 A total of 152 water samples from QCS, JZ, and LH reservoirs were collected for molecular de-
114 tection, respectively. The 500 mL subsamples were filtered by 1.2 µm Isopore™ Membrane
115 Filters, then the membrane filters were stored at -20 °C in 1.5 mL centrifuge tubes until DNA
116 and RNA extraction. The DNA and RNA of water samples were extracted using the Fast DNA™
117 spin kit for soil (MP Biomedicals, USA) and E.Z.N.A.™ Soil RNA Kit (OMEGA, USA), respectively.
118 PrimeScript™ RT Master Mix (TaKaRa, Japan) was used to reverse transcribe RNA to cDNA, per-
119 forming the reaction at 37 °C for 15 min followed by 85 °C for 5 s. The concentration and purity
120 of DNA and cDNA were identified by microspectrophotometry (NanoDropND-2000, NanoDrop
121 Technologies, Willmington, DE). DNA and cDNA samples were stored at -80 °C until use.

122 2.3. Quantification of *mic* gene

123 The primers MIBQSF (5'-GACAGCTTCTACACCTCCATGA-3') and MIBQSR (5'-CAA TCTGTAGCACCATGTTGAC-
124 3') were used to amplify the cyanobacterial *mic* gene (Suruzzaman et al., 2022). The quantitative
125 PCR was carried out in a 25 µL volume mixture including 12.5 µL TB Green™ Premix Ex Taq™
126 (TaKaRa, Japan), 0.8 µL for each primer (MIBQSF and MIBQSR), 8.9 µL deionized water, and 2
127 µL template DNA. The quantitative PCR was conducted using LightCycler 96 (Roche, USA), and
128 the reaction conditions were pre-incubation at 95 °C for 10 min; 50 cycles at 95 °C for 20 s,
129 50 °C for 20 s, and 72 °C for 20 s; and DNA melting from 65 °C to 97 °C. The specification of
130 qPCR amplification protocol was verified using 12 MIB-producing cyanobacteria and 5 non-MIB
131 producing cyanobacteria, no non-specific amplicon was found in gel image (Suruzzaman et al.,
132 2022). Standard curves were obtained by dilution from linearized plasmids containing between
133 10^{10} and 10^4 *mic* gene copies μL^{-1} , and all the measurements were conducted in triplicate. The

134 standard curve was obtained: $C_q = -3.4537lg(c_{mic}) + 40.13(R^2 = 0.999, p < 0.0001)$
135 with the efficiency of 95% (Fig. S3). Negative control was used to distinguish the specific and
136 non-specific amplification (Fig. S4).

137 2.4. Identification of MIB producers

138 We combined multiple methods including high-throughput sequencing and pure culture to
139 identify the MIB producers in QCS Reservoir. Firstly, considering the cyanobacteria and actino-
140 mycetes have the potential to produce MIB in natural water bodies but they have different gene
141 order in MIB operon (Devi et al., 2021), the genetic information of *mic* genes can be used to
142 identify the MIB producers. Here, nanopore sequencing (with long reads that can span the MIB
143 operon (about 5000 bp)) was used to investigate the genetic environment of *mic* genes in QCS
144 Reservoir and further identify the MIB contribution of cyanobacteria or actinomycetes. Environ-
145 mental DNA was prepared for library construction, large DNA fragments were recovered using
146 the BluePippin automatic nucleic acid recovery system (Sage Science), and then purified using
147 magnetic beads. The two ends of purified DNA were repaired and connectors were added. These
148 constructed libraries were sequenced on the Oxford Nanopore Technology (ONT) platform. Raw
149 data were preprocessed by Trimmomatic (v.0.36) to obtain clean data. Further, the clean data
150 were mixed and assembled to Scaffigs using MEGAHIT (v.1.0.6), then the Scaffigs shorter than
151 500 bp were filtered for subsequent analysis. The *mic* gene in the Scaffigs was determined by
152 BLASTN with *mic* gene sequences obtained from the National Center for Biotechnology Infor-
153 mation (NCBI) GenBank. The sequencing data were submitted to the NCBI BioProject database
154 with accession number PRJNA844292.

155 In addition, sequencing of the *mic* genes of environmental DNA can provide clues to explore
156 the communities of potential MIB producers (Qiu et al., 2021). The primers MIBQSF
157 (5'-GACAGCTTCTACACCTCCATGA-3') and MIBQSR (5'-CAATCTGTAGCACCATGTTGAC-3') with bar-
158 code sequences at two ends were used to amplify the *mic* genes of environmental samples (Su-
159 ruzaman et al., 2022). Purified amplicons were paired-end sequenced on the Illumina MiSeq
160 PE300 platform (Illumina Inc., San Diego, USA). Paired-end reads were merged by the FLASH

161 program (Magoc and Salzberg, 2011). Then the sequences were clustered to operational tax-
162 onomic units (OTUs) by UPARSE with 97% similarity cutoff (Edgar, 2013), and the singletons
163 and chimeras were removed. Representative sequences of OTUs were blasted with *mic* gene
164 sequences obtained from the National Center for Biotechnology Information (NCBI) GenBank
165 to identify the contributors to *mic* genes. The sequencing raw data were submitted to NCBI
166 BioProject database with accession number PRJNA838781.

167 Finally, the potential MIB producers were isolated and their MIB production abilities were
168 confirmed. A single filament was picked up under the microscope and washed with sterile
169 ddH₂O several times until the only target filament was obtained. The isolated *Pseudan-*
170 *abaena* were cultured under 25 °C and light intensity of 30 μmol photons m⁻² s⁻¹ in BG11
171 medium. GC-MS was used to identify the MIB production abilities of these isolated strains.
172 Taxonomic classification was confirmed by 16S rRNA gene sequencing, with the primers 27F
173 (5'-AGAGTTTGATCCTGGCTCAG-3') and 1492R (5'-TACGGCTACCTGTTACGACTT-3'). Three strains
174 of *Pseudanabaena* were isolated from MIB episode water samples in QCS Reservoir.

175 2.5. Culture experiment for *Pseudanabaena*

176 *Pseudanabaena cinerea* FACHB 1277 obtained from the Freshwater Algae Culture Collection
177 at the Institute of Hydrobiology was used to investigate the effects of light intensity on the cell
178 growth, MIB production, and *mic* gene expression level during the culture period of 35 days.
179 Cells of *Pseudanabaena* in the logarithmic growth phase were centrifuged (1000 RPM, 2 min)
180 and washed 3 times with BG11 medium to remove the extracellular odorous substances. The
181 subsequent culture experiments were performed at a cell density of approximately 2×10^6 cells
182 L⁻¹ based on the cell concentrations observed in QCS Reservoir during the field investigation.

183 *Pseudanabaena* were cultured in triplicate at 25 °C under a 12 h/12 h light/dark cycle in 30
184 mL BG11 medium, under different light intensities of 5, 17, 36, 85, and 250 μmol photons m⁻²
185 s⁻¹, respectively, according to the variations of light intensities in QCS Reservoir during the MIB
186 episode (15.7 ~ 51.1 μmol m⁻²s⁻¹).

187 2.6. Statistical analysis

188 Non-metric multidimensional scaling analysis (NMDS) was first proposed by Kruskal (1964),
189 and have been extensively used to explore the temporal and spatial transitions of phytoplankton
190 communities with in Primer v7 ((Clarke and Gorley, 2015)), and the differences between the com-
191 munities were tested using the permutational multivariate analysis of variance (PERMANOVA,
192 (Anderson, 2017)) with 9999 permutations by the Bray-Curtis dissimilarity matrix, performed by
193 the vegan package (Dixon, 2003) based on R language (R Core Team, 2020). The advance days
194 of the *mic* gene-based early warning method were determined by conducting time-shifted pair-
195 wise Pearson's correlation analysis. The correlations between MIB concentration and *mic* gene
196 (DNA and RNA) abundance were screened with different lag days (Δd) from 0 to 14. The lag day
197 with the highest correlation was further determined as the advance time for early warning of
198 the MIB episode.

199 The underwater light intensity in QCS Reservoir is determined by solar irradiance and mixing
200 characters of reservoir water, and can be calculated by (Eq. 1) as follows:

$$I_c = I_u \frac{1 - e^{-kz_{mix}}}{kz_{mix}} \quad (1)$$

201 Where I_u is the sub-surface solar irradiance, k is the light extinction coefficient, and z_{mix} is
202 the mixing depth. Considering the well-mixed characteristics of the water body in QCS Reservoir,
203 z_{mix} is equivalent to the water depth (z_{max}).

204 Regarding the culture experiment, the cell growth rate at the logarithmic phase (μ , d^{-1}) was
205 calculated based on the cell density increase (N_{t_2}/N_{t_1}) over time ($t_2 - t_1$, d) (Eq. 2), which
206 was determined by the slope of log-linear model between N_t and t .

$$\mu = \frac{\ln N_{t_2} - \ln N_{t_1}}{t_2 - t_1} \quad (2)$$

207 The instantaneous cellular MIB yield ($Y_t = c_t/N_t$) was determined according to the instant

208 total MIB concentration (c_t , including cell-bound MIB and dissolved MIB) and cell density (N_t).
209 The mean cellular MIB yield (Y) was determined according to the mean of all instantaneous
210 cellular MIB yields within the late logarithmic phase and stationary phase for each experiment
211 set. Linear regression, one-way analysis of variance (ANOVA), and Pearson's correlations were
212 performed by the vegan package (Oksanen et al., 2014). The figures were visualized using the
213 ggplot2 package (Wickham, 2009) and ArcGIS v.10.7.

214 3. Results

215 3.1. Limnological characteristics

216 Seasonal MIB episodes lasting for one to two months have been typically observed in the pe-
217 riod from Apr. and Jun. in QCS Reservoir since 2016, according to the historical record (data not
218 shown). In 2021, the MIB episode started in the end of April, and ended in late May 25. The
219 solar irradiance varied between $210.6 \mu\text{mol photons m}^{-2} \text{s}^{-1}$ and $761.8 \mu\text{mol photons m}^{-2} \text{s}^{-1}$ (Fig.
220 S5), meanwhile, the underwater light intensity varied between $15.7 \mu\text{mol photons m}^{-2} \text{s}^{-1}$ and
221 $51.1 \mu\text{mol photons m}^{-2} \text{s}^{-1}$. The air temperature was $21.6 \text{ }^\circ\text{C}$ and showed $4.4 \text{ }^\circ\text{C}$ variance. In
222 comparison, the water temperature showed a much smaller variance of $1.8 \text{ }^\circ\text{C}$ with mean value
223 of $20.2 \text{ }^\circ\text{C}$ during the episode in 2021 (Fig. S5), and no significant spatial difference between
224 Upstream river water (URW) and reservoir water was observed ($p = 0.631$). The water level was
225 $2.48 \pm 0.25 \text{ m}$ and hydraulic retention time was $16.7 \pm 4.9 \text{ d}$. The dissolved oxygen (DO), pH, and
226 secchi depth (SD) in URW were significantly lower than those in reservoir water ($p < 0.01$), while
227 the turbidity, total phosphorus (TP), total nitrogen (TN), and nitrate ($\text{NO}_3\text{-N}$) in URW were signif-
228 icantly higher ($p < 0.01$). No significant spatial difference was observed for ammonia ($\text{NH}_4\text{-N}$, p
229 $= 0.096$).

230 In 2021, a rapid increase in MIB occurred at the end of Apr. and peaked in the middle of May
231 with the highest concentration (99.0 ng L^{-1}) detected at QC10 on May 10, and subsequently it
232 decreased to below the odor threshold (10.0 ng L^{-1}) on May 25 (Fig. 1). No serious MIB problem
233 was observed in upstream river water (URW) and the south branch (SB) of the reservoir. MIB

Table 1 Limnological characteristics in QCS Reservoir during the investigation. The values are expressed as means and standard deviations

I	T _{air}	Wind	Rainfall	Water level	HRT
($\mu\text{mol m}^{-2}\text{s}^{-1}$)	(°C)	(m s^{-1})	(mm d^{-1})	(m)	(d)
607 ± 179	21.6 ± 4.4	2.93 ± 1.55	4.34 ± 11.57	2.48 ± 0.25	16.7 ± 4.9

Parameters	URW	NB	SB	MS	Sig.
T _{water} (°C)	20.2 ± 1.8	20.3 ± 1.8	20.4 ± 1.6	20.0 ± 1.9	0.631
DO (mg L^{-1})	8.7 ± 0.6	9.2 ± 1.2	8.8 ± 1.0	9.6 ± 0.8	0.000
pH	8.2 ± 0.07	8.7 ± 0.1	8.3 ± 0.2	8.6 ± 0.1	0.000
SD (cm)	41 ± 14	65 ± 18	44 ± 9	77 ± 17	0.000
Turb. (NTU)	52.2 ± 39.9	10.6 ± 4.9	18.3 ± 6.0	8.2 ± 3.2	0.000
TP (mg L^{-1})	0.09 ± 0.03	/	/	0.05 ± 0.01	0.000
TN (mg L^{-1})	1.96 ± 0.09	/	/	1.61 ± 0.11	0.000
Nitrate (mg L^{-1})	1.77 ± 0.08	/	/	1.37 ± 0.09	0.000
Ammonia (mg L^{-1})	0.07 ± 0.02	/	/	0.06 ± 0.02	0.096
MIB (ng L^{-1})	1.3 ± 0.5	22.1 ± 22.6	3.7 ± 5.3	20.5 ± 18.5	0.000

234 concentrations at the middle section (MS) and the north branch (NB) were significantly higher
 235 than those of URW ($p < 0.01$) and SB ($p < 0.01$).

236 3.2. Dynamics of phytoplankton community structure

237 A total of 21 cyanobacterial genera and 55 genera affiliated with 6 other phyla were recorded
 238 during the investigation according to microscopic cell counting results. The phytoplankton com-
 239 munities showed significant temporal (PERMANOVA, $R^2 = 0.14$, $F = 2.988$, $p < 0.001$) and spatial
 240 (PERMANOVA, $R^2 = 0.13$, $F = 1.846$, $p = 0.015$) differences (Fig. S6). Cyanophyta and Bacillario-
 241 phyta were the two dominant phyla over the investigation period from Apr. to Jun. The abun-
 242 dance of Cyanophyta peaked on May 10 (4.4×10^6 cells L^{-1}), but decreased quickly to (1.0×10^6)
 243 cells L^{-1} on May 17, leaving Bacillariophyta ($(3.0 \pm 1.0) \times 10^6$ cells L^{-1}) and Chlorophyta ((9.4 ± 8.0)
 244 $\times 10^5$ cells L^{-1}) as the dominant phyla (Fig. 2B). The cell density of *Pseudanabaena*, a well-known
 245 potential MIB producer, increased from Apr.19 (4.6×10^5 cells L^{-1}) to May 12 (4.8×10^6 cells L^{-1}),
 246 then decreased to (1.3×10^5 cells L^{-1}) on May 21 (Fig. 2A), exhibiting a similar temporal pattern

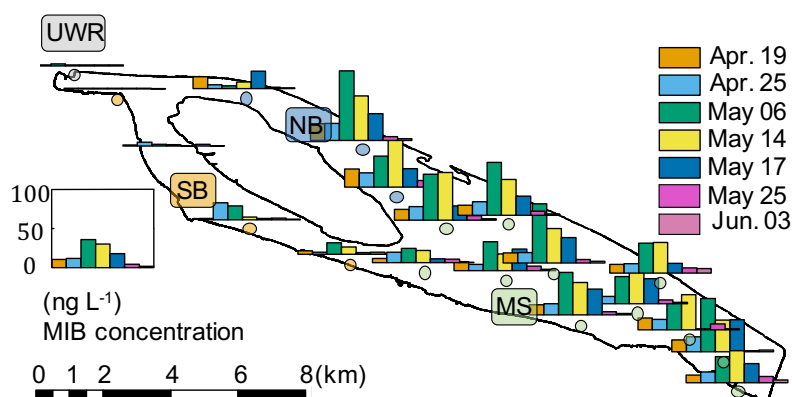


Fig. 1 The spatial and temporal distributions of MIB concentrations during the MIB episode of QCS Reservoir in 2021.

247 as the MIB concentration ($R^2 = 0.28$, $p < 0.01$, Fig. S7).

248 The *mic* gene was detected in 133 water samples collected from QCS Reservoir during the
 249 MIB episode. The genes' order in the MIB operon was determined as illustrated in Fig. 2C. The
 250 *mic* gene was located between the *mtf* gene and *cnb B* gene, suggesting that MIB was pro-
 251 duced by the cyanobacteria (Devi et al., 2021). The *mic* gene sequences were subsequently
 252 determined to explore the potential MIB producers together with microscopic results. *Pseu-*
 253 *danabaena* was identified as the dominant MIB contributor (accounting for 82.7% of the MIB-
 254 producing cyanobacterial community) by the annotation of *mic* gene sequences (Fig. 2C); *Oscilla-*
 255 *toria*, at the same time, contributed 5.1%. Furthermore, 3 *Pseudanabaena* strains were isolated
 256 from the QCS water samples, with *Pseudanabaena cinerea* being determined as the main MIB
 257 producer in QCS Reservoir according to the MIB production potential test (Table S2).

258 3.3. Correlation between MIB concentration and *mic* gene abundance

259 The spatial and temporal patterns of *mic* gene abundances (DNA and RNA) are shown in Fig. 3A,
 260 which agreed well with the MIB distribution. The *mic* gene abundances (DNA or RNA) of NB and
 261 MS were significantly higher than UWR ($p < 0.01$) and SB ($p < 0.01$). In general, DNA reached the
 262 peak values earlier than RNA.

263 Daily samples at NB (QC10) were further analyzed to reveal the temporal dynamics of the total

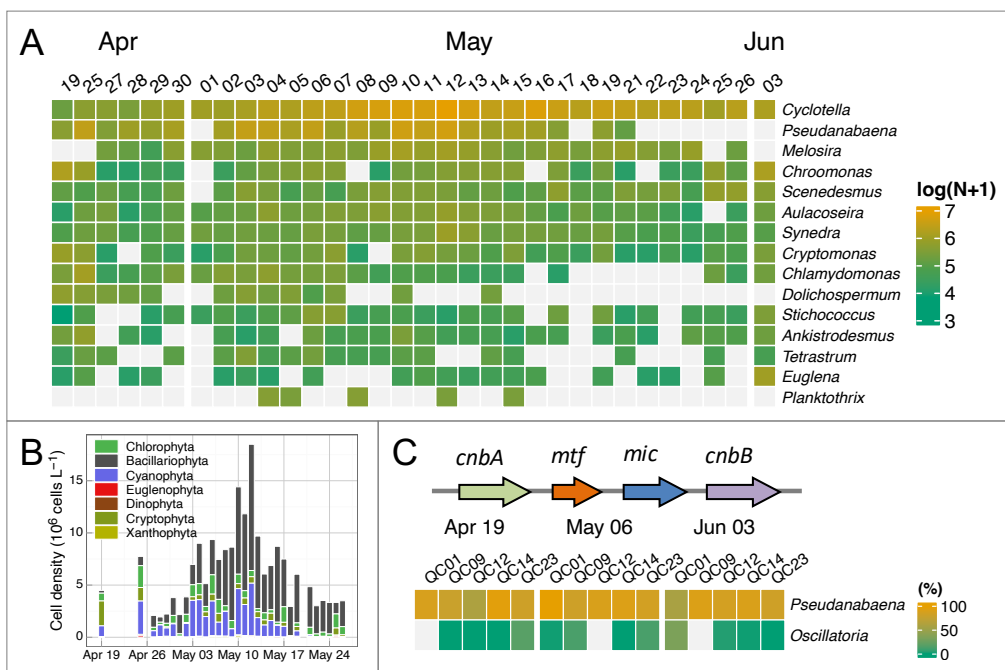


Fig. 2 Cyanobacterial community (obtained by microscopic cell counting) in QCS Reservoir at the genus level (top 20% genera, A), the *mic* gene order (B) and proportion of relative abundances of MIB-producing cyanobacteria determined by *mic* gene sequencing (C).

264 MIB concentrations and *mic* gene abundances (DNA and RNA). The highest MIB concentration
 265 (99 ng L^{-1} , Fig. 3C) was detected on May 10, while the highest DNA ($3.67 \times 10^7 \text{ copies L}^{-1}$, Apr. 30)
 266 and RNA ($2.03 \times 10^7 \text{ copies L}^{-1}$, May 3) abundances of the *mic* gene occurred earlier than the
 267 peak MIB concentration (Fig. 3B).

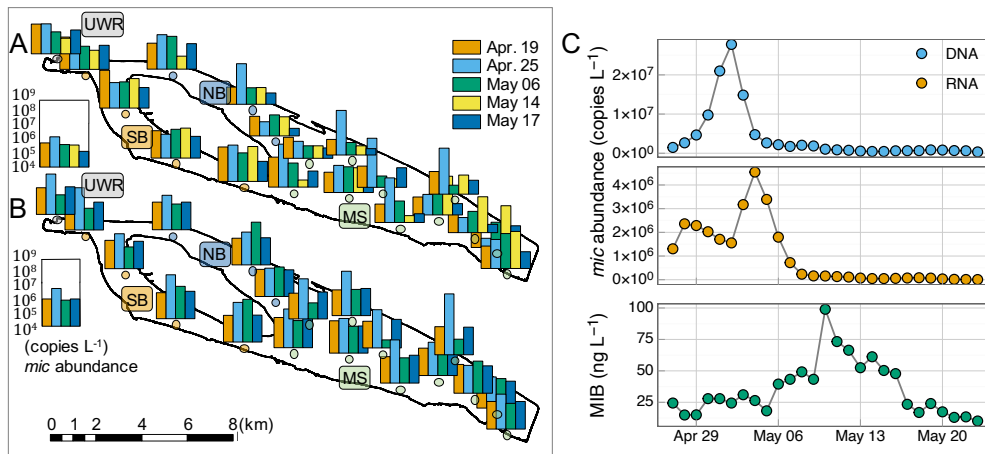


Fig. 3 Spatial and temporal distribution of DNA (A, top) and RNA (A, bottom) abundance of *mic* gene during the MIB episode in QCS Reservoir, and the temporal dynamics of gene abundance (B) and MIB concentration (C) at QC10.

268 Time-shifted pairwise Pearson's correlation analysis was performed to evaluate the lag time
 269 between *mic* gene abundance and MIB concentration. The highest correlations with MIB con-
 270 centration were obtained at 10 lag days for DNA and 7 lag days for RNA, respectively (Fig. 4A).
 271 Furthermore, RNA abundance of *mic* gene ($R^2 = 0.45$, $p < 0.01$, Fig. 4C) showed a little higher
 272 correlation with MIB concentration than the DNA abundance ($R^2 = 0.37$, $p < 0.01$, Fig. 4B). The
 273 mean *mic* gene quota (MIB production per *mic* gene copy) was 33 and 181 (fg / *mic* gene copy)
 274 for DNA and RNA, respectively.

275 The earlier peak of *mic* gene abundance compared to MIB concentration was also observed in
 276 JZ Reservoir and LH Reservoir. In JZ Reservoir, The highest DNA abundance ($5.02 \times 10^5 \text{ copies L}^{-1}$)
 277 and MIB concentration (147 ng L^{-1}) were detected on Aug. 5 and Aug. 20, respectively. Similar
 278 result has been found in LH Reservoir, the highest DNA abundance ($7.32 \times 10^6 \text{ copies L}^{-1}$) and
 279 MIB concentration (72 ng L^{-1}) were detected on May 23 and Jun. 14, respectively.

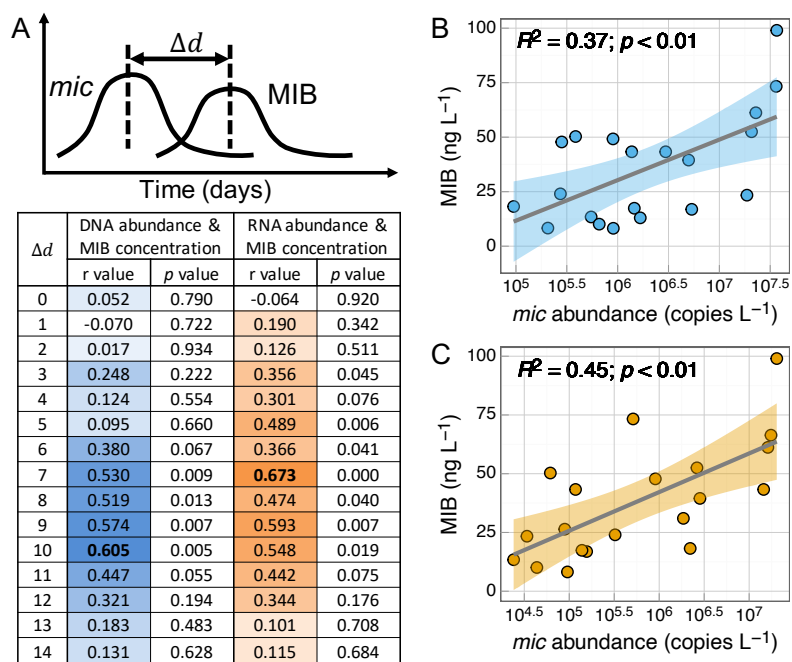


Fig. 4 Time-shifted pairwise Pearson's correlation between MIB concentration and DNA or RNA (A) abundances of *mic* gene at QC10. The correlation coefficients were scanned with different lag days (Δd) from 0 to 14. The best correlation between MIB concentration and DNA (B) and RNA (C) abundances of *mic* gene.

280 3.4. Driving factors for *mic* gene expression

281 Driving factors responsible for *mic* gene expression were explored to reveal the differences
282 in the temporal variations between the DNA and RNA abundances of *mic* gene during the MIB
283 episode. Water temperature and nutrients were excluded as the major driving factors since
284 no correlation was obtained with *mic* gene abundances (Fig. S9). Only the light intensity was
285 positively correlated with the RNA abundance of *mic* gene ($R^2 = 0.44$, $p < 0.01$, Fig. 5B), though
286 no correlation was observed with DNA abundance ($R^2 = 0.02$, $p = 0.64$, Fig. 5A).

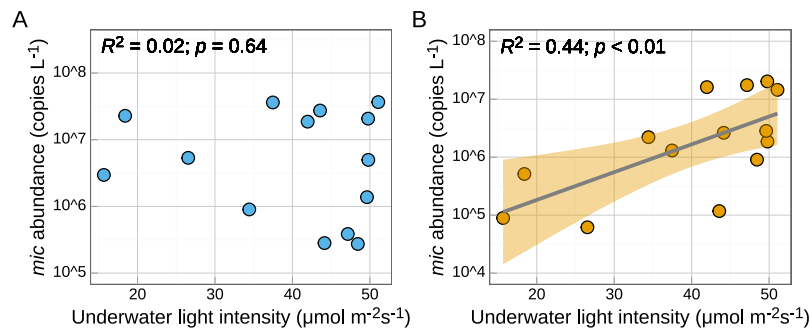


Fig. 5 Correlation between mean underwater light intensity and DNA (A) or RNA (B) abundances of *mic* gene, respectively, at QC10 during the MIB episode.

287 Further, a culture experiment using *Pseudanabaena cinerea* FACHB 1277 (the major contribu-
288 tor to MIB in QCS Reservoir) was performed to investigate the effects of light intensity on cell
289 growth, MIB production, and *mic* gene expression level (Fig. 6). The highest cell growth rate
290 (0.26 ± 0.03) d^{-1} was obtained under moderate light intensity ($36 \mu\text{mol photons m}^{-2} \text{s}^{-1}$). Mean-
291 while, the maximum cell density (1.3 ± 0.3) $\times 10^{10}$ cells L^{-1} and MIB concentration (897 ± 75) μg
292 L^{-1} were also observed at $36 \mu\text{mol photons m}^{-2} \text{s}^{-1}$.

293 Different from the optimum light intensity for cell growth, the maximum cellular MIB yield
294 (0.15 ± 0.04) pg cell^{-1} was achieved at $85 \mu\text{mol photons m}^{-2} \text{s}^{-1}$. The expression level of *mic* gene
295 (normalized by cell density) was roughly stable along the culture period under a certain light
296 intensity, but responded to diverse light intensities. The *mic* gene expression level increased
297 by 50 % under $85 \mu\text{mol photons m}^{-2} \text{s}^{-1}$ compared to $36 \mu\text{mol photons m}^{-2} \text{s}^{-1}$, but higher light

298 intensity ($250 \mu\text{mol photons m}^{-2} \text{s}^{-1}$) could inhibit the *mic* gene expression (Fig. 6E).

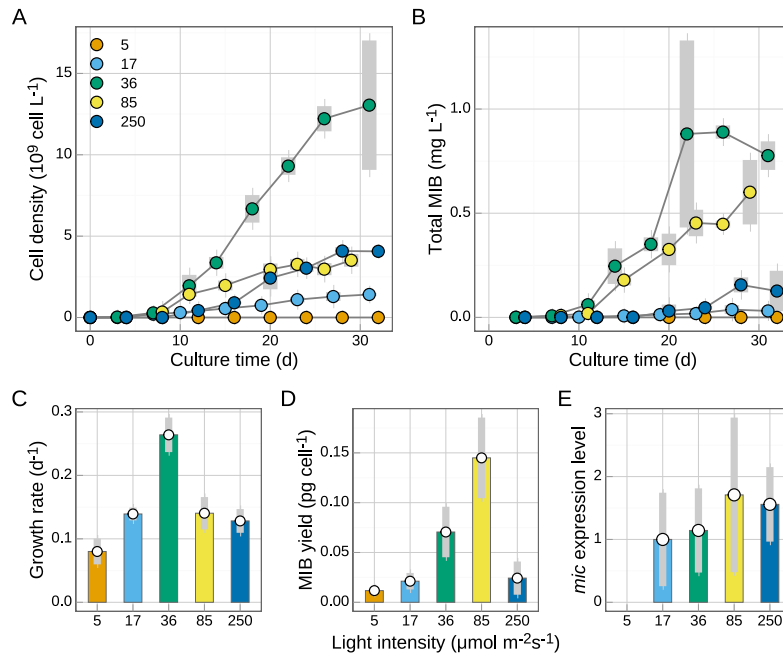


Fig. 6 Cell density (A), total MIB production (B), cell growth rate (C), cellular MIB yield (D), and *mic* gene expression level (normalized by cell density) (E) of *Pseudanabaena cinerea* FACHB 1277 under different light intensities.

299 4. Discussion

300 4.1. MIB episodes in QCS Reservoir

301 Widespread musty odor events caused by MIB have been increasingly reported in recent
 302 decades, raising considerable public attention (Lee et al., 2017; Devi et al., 2021). Cyanobacteria
 303 (Lee et al., 2017) and actinomycetes (Zaitlin and Watson, 2006; Zuo et al., 2010) have been
 304 widely accepted as the main MIB producers, although the dominant source for a specific water
 305 body is sometimes controversial. Previous studies have revealed that the cyclic nucleotide-
 306 binding protein genes (*cnb A* and *cnb B*), methyl transferase gene (*mtf*), and MIB cyclase gene
 307 (*mic*) are associated with MIB biosynthesis (Giglio et al., 2011; Komatsu et al., 2008). The order
 308 of these genes within cyanobacteria (*cnbA* - *mtf* - *mic* - *cnbB*) is different from that in most of

309 the actinomycetes (*cnb - mic - mtf*) because of the occurrence of recombinant events during
310 evolution (Devi et al., 2021). In QCS Reservoir, the genes' order in the MIB operon (*cnbA*,
311 followed by *mtf*, *mic*, and *cnbB*) indicates that cyanobacteria are the major contributor to the
312 MIB episode.

313 All of the microscopic, high-throughput sequencing and pure culture results revealed that *Pseu-*
314 *danabaena cinerea* was the dominant MIB producer in 2021, though *Oscillatoria* might have also
315 contributed slightly to the MIB episode. Previous studies in general only focused on one MIB
316 producer for a specific MIB episode (Su et al., 2021; Huang et al., 2018). This study shows that
317 the ecological niche in QCS Reservoir could support two MIB-producing genera. The dominant
318 MIB-producing species may be different in different years since the environmental conditions
319 may change. At the same time, it should be noted that there were also two other *Pseudan-*
320 *abaena* species (*P. limnetica* and *P. catenate*) which could not produce MIB, which is easy to
321 understand since the same genera usually favor similar niches. This study clearly shows that
322 microscopic identification alone (Fig. S8) is therefore not sufficient to identify the MIB produc-
323 ers, considering the co-occurrence of MIB-producing *Pseudanabaena* and non-MIB producing
324 *Pseudanabaena*, and the cell lysis when MIB release.

325 4.2. Early warning of MIB episode based on *mic* gene abundance and expression

326 Quantification of MIB synthesis genes has been regarded as a sensitive and rapid method for
327 the evaluation of the MIB production potential in drinking water sources (Chiu et al., 2016; Kim
328 et al., 2020; Lu et al., 2019; Rong et al., 2018; Wang and Li, 2015), which can be completed within
329 one day from samples collection to result analysis, and the cost is lower than GC-MS analysis.
330 This study clearly demonstrates for the first time that the detection of the *mic* gene could be used
331 as an effective early warning approach for an MIB episode since the peaks of the DNA and RNA
332 abundances arrived 10 and 7 days earlier than that of MIB concentration. The *mic* gene has been
333 reported as single copy in the genome of *Pseudanabaena*, *Planktothricoides* and the majority of
334 actinomycetes (Giglio et al., 2011; Komatsu et al., 2008; Wang et al., 2011), indicating a consis-
335 tent correlation between *mic* gene abundance and *P. cinerea* cell density. Moreover, early total

336 *Pseudanabaena* abundance increases were observed before May 10 according to microscopic
337 cell counting, suggesting *P. cinerea* probably the dominant *Pseudanabaena* species in the early
338 stage. Since intracellular MIB is mainly released into water during the stationary/death phase
339 (Alghanmi et al., 2018), we speculate that the massive breakdown of *P. cinerea* cells before May
340 10 resulted in the instant MIB increases in QCS Reservoir. In addition, the transportation and dif-
341 fusion processes of MIB were also important reasons for the 7 ~ 10 days' delay of MIB episodes
342 in comparison with the dynamics of *mic* gene abundance. Previous studies showed that short hy-
343 draulic retention time (HRT) could inhibit cyanobacterial growth via disrupt and dilute processes,
344 and HRT was positively correlated with cyanobacterial abundance (Lee et al., 2012; Rangel et al.,
345 2012). Further study is still required to obtain the relationship between hydrodynamics and the
346 time lag.

347 This real-time PCR-based approach is particularly important considering the fact that only one
348 among the three *Pseudanabaena* strains isolated from the episode samples exhibited the po-
349 tential to produce MIB. If the waterworks could predict the occurrence of the peak MIB con-
350 centrations 7 or 10 days earlier, they could have sufficient time to take measures to cope with
351 the episode. They can change the source water, regulating the flow rate, preparing PAC for MIB
352 removal, or reduce the problematic source water to ensure sufficient adsorption time since the
353 adsorption of MIB mainly occurs in the micropores of PAC, requiring long adsorption time (Yu
354 et al., 2007).

355 Since the *mic* gene is essential for MIB production regardless of taxonomy, this method can
356 be applied to all MIB episodes. Though the RNA-based gene abundance ($R^2 = 0.44$) is slightly
357 more accurate than the DNA-based one ($R^2 = 0.37$), DNA detection may be a more practical
358 approach since the detection of DNA is easier, and the advance time (10 days) is longer. This
359 advance time was in accordance with a previous study on microcystin production (7 days; (Lu
360 et al., 2020)). The *mic* gene-based early warning function was also validated by application in
361 2 drinking water reservoirs (JZ Reservoir and LH Reservoir, Fig. S12). Both applications exhib-
362 ited an earlier peak of *mic* gene abundance compared to the MIB concentration, though the
363 advance days cannot be accurately confirmed due to the low sampling frequency. This further

364 supports the validation of this technology for early warning purpose, although the number of
365 advance days should be adjusted before application due to physiological differences between
366 MIB producers and differences in the hydrodynamics of reservoirs/lakes.

367 4.3. Driving factors for MIB production

368 MIB production in actual water is governed by the growth of MIB producer(s), the expression
369 level of MIB synthesis gene and hydrological transportation of MIB diffusion. As a result, the cor-
370 relation between observed MIB concentration and abundance of MIB producer(s) is not strong,
371 e.g., in this study the correlation coefficient between *Pseudanabaena* cell density and MIB con-
372 centration is 0.28, and the MIB concentration can only be modeled using quantile regression in
373 Miyun Reservoir (Su et al., 2015). It suggests that the gene expression should be emphasized.
374 Noted that, RNA abundance of *mic* gene is a better indicator of MIB dynamics compared to DNA
375 abundance, with 8% variance differences, indicating that the *mic* gene expression is governed
376 by other factors during the MIB episode.

377 Water temperature, nutrients and light availability have been considered to be key factors af-
378 fecting the growth and MIB production of cyanobacteria. For *Pseudanabaena*, higher tempera-
379 ture could promote cell growth (25-35 °C), MIB production (Izaguirre and Taylor, 2007; Wang and
380 Li, 2015; Zhang et al., 2016) and *mic* gene expression (30 °C) (Kakimoto et al., 2014). However,
381 no significant correlation between water temperature and *mic* gene abundances (DNA or RNA)
382 was observed in QCS Reservoir, probably owing to the small temperature variations (17.2 °C to
383 26.0 °C) during the MIB episode. The uncorrelated relationship between nutrients concentra-
384 tion and *mic* gene abundances (DNA and RNA) in QCS Reservoir further supports that nutrients
385 are probably not the key factor governing *mic* gene expression. Nutrients are generally not the
386 limiting factor for MIB producers, as they prefer to stay in the subsurface/bottom layers of the
387 water column, where nutrients from sediments can satisfy their demand (Su et al., 2019, 2021),
388 which is why prevalent MIB episodes usually occur in mesotrophic/oligotrophic reservoirs/lakes
389 (Su et al., 2019).

390 Cyanobacteria capture light photons by using photosynthetic pigments including chlorophyll *a*
391 and phycobillins through photosynthesis (Wiltbank and Kehoe, 2019). MIB biosynthesis shares
392 a common precursor with chlorophyll *a* (Zimba et al., 1999), therefore the ambient light con-
393 dition probably is an essential regulator that governs the cell growth (indicator of chlorophyll
394 *a* biosynthesis) and MIB production for cyanobacteria, as also observed in other culture exper-
395 iments (Jia et al., 2019; Li et al., 2012; Wang and Li, 2015; Su et al., 2023). Our culture result
396 indicates that *Pseudanabaena* cannot grow under light intensity as low as 5 $\mu\text{mol photons m}^{-2}$
397 s^{-1} , consistent with Zhang et al. (2016); optimized growth was obtained under 36 $\mu\text{mol photons}$
398 $\text{m}^{-2} \text{s}^{-1}$, but maximum cellular MIB production was obtained under 85 $\mu\text{mol photons m}^{-2} \text{s}^{-1}$. This
399 result is also consistent with Zhang et al. (2016), showing that the optimum light intensities for
400 cell growth and MIB production were 25 and 40 $\mu\text{mol photons m}^{-2} \text{s}^{-1}$, respectively. The *mic*
401 gene expression was promoted along with the increase in light intensity from 17 to 85 μmol
402 $\text{photons m}^{-2} \text{s}^{-1}$, resulting in incremental cellular MIB yield. Nevertheless, the level of *mic* gene
403 expression in response to light is strain-specific according to comparison with another indepen-
404 dent study (Wang et al., 2011), which revealed that the *mic* gene expression of *Pseudanabaena*
405 sp. dqh15 was inhibited under 60 $\mu\text{mol m}^{-2} \text{s}^{-1}$ compared to 30 $\mu\text{mol m}^{-2} \text{s}^{-1}$.

406 Meanwhile, the mean underwater light intensity varied between 15.7 and 51.1 $\mu\text{mol photons}$
407 $\text{m}^{-2} \text{s}^{-1}$ during the MIB episode in QCS Reservoir (Fig. S10). It is interesting that the light intensity
408 was positively correlated with the *mic* gene abundance of RNA ($R^2 = 0.44$, $p < 0.01$), but not
409 with DNA ($R^2 = 0.02$, $p = 0.64$). It is possible that the light fluctuation during the MIB episode
410 was not big enough to affect the cell growth of *Pseudanabaena*. However, the result clearly
411 shows that the *mic* gene expression was more sensitive to underwater light intensity than was
412 cell growth, which was in accordance with the pure culture experiment. In QCS Reservoir, the
413 relatively higher light intensity ($46.3 \pm 5.1 \mu\text{mol photons m}^{-2} \text{s}^{-1}$) during the period Apr. 29 to
414 May 3 may have caused the observed increase in MIB concentration 7 days later (from May 6
415 to May 10, Fig. S10). This light response feature of *Pseudanabaena* means that the production
416 of MIB may be greatly reduced even for abundant MIB producers if the light availability is not
417 favorable for the expression of the *mic* gene. Therefore, although the detection of DNA is used

418 for early warning of the MIB episode, the detection of RNA is also desirable for a more accurate
419 prediction, and the light intensity should be also an important predictor.

420 **5. Conclusion**

421 According to investigation of an MIB episode in QCS Reservoir, and a culture experiment for
422 *Pseudanabaena cinerea*, the following conclusions can be drawn. 1) *P. cinerea* was identified as
423 the major MIB producer in QCS Reservoir during the investigation in 2021. 2) *mic* gene expres-
424 sion level is light dependent, in particular, relatively higher light intensity results in increasing
425 cellular MIB yield when underwater light intensity is proper for their growth. 3) The *mic* DNA
426 abundance and expression can be used for early warning purpose with 7 ~ 10 days forecasts,
427 offering a valuable time gap for control measures and emergency operation.

428 **6. Notes**

429 The authors declare no competing financial interest.

430 **Acknowledgements**

431 This work was financially supported by the National Natural Science Foundation of China
432 (51878649, 52030002), Shanghai Chengtuo Raw Water Co. Ltd., and Youth Innovation
433 Promotion Association CAS.

434 **References**

- 435 Alghanmi, H.A., Alkam, F.M., AL-Tae, M.M., 2018. Effect of light and temperature on new cyanobacteria producers for
436 geosmin and 2-methylisoborneol. *Journal of Applied Phycology* 30, 319–328. URL: <https://doi.org/10.1007/s10811-017-1233-0>, doi:10.1007/s10811-017-1233-0.
- 437
438 Anderson, M.J., 2017. Permutational multivariate analysis of variance (PERMANOVA). URL: [https://doi.org/10.1002/](https://doi.org/10.1002/2F9781118445112.stat07841)
439 [2F9781118445112.stat07841](https://doi.org/10.1002/9781118445112.stat07841), doi:10.1002/9781118445112.stat07841.

440 Chiu, Y., Yen, H., Lin, T., 2016. An alternative method to quantify 2-MIB producing cyanobacteria in drinking water
441 reservoirs: Method development and field applications. *Environmental Research* 151, 618–627. URL: <http://www.sciencedirect.com/science/article/pii/S0013935116305059>, doi:10.1016/j.envres.2016.08.034.

442

443 Clarke, K., Gorley, R., 2015. Primer v7: User Manual/Tutorial.

444 Cook, D., Newcombe, G., Sztajn bok, P., 2001. The application of powdered activated carbon for MIB and geosmin
445 removal: predicting PAC doses in four raw waters. *Water Research* 35, 1325–1333. URL: [https://doi.org/10.1016/S0043-1354\(00\)00363-8](https://doi.org/10.1016/S0043-1354(00)00363-8), doi:10.1016/S0043-1354(00)00363-8.

446

447 Devi, A., Chiu, Y.T., Hsueh, H.T., Lin, T.F., 2021. Quantitative pcr based detection system for cyanobacterial geosmin/2-
448 methylisoborneol (2-MIB) events in drinking water sources: Current status and challenges. *Water Research* 188,
449 116478. URL: <https://www.sciencedirect.com/science/article/pii/S0043135420310137>, doi:10.1016/j.watres.
450 2020.116478.

451 Dixon, P., 2003. VEGAN, a package of r functions for community ecology. *Journal of Vegetation Science* 14, 927–930.
452 URL: <https://doi.org/10.1111%2Fj.1654-1103.2003.tb02228.x>, doi:10.1111/j.1654-1103.2003.tb02228.x.

453 Edgar, R.C., 2013. UPARSE: highly accurate OTU sequences from microbial amplicon reads. *Nature Methods* 10, 996–998.
454 URL: <https://doi.org/10.1038/nmeth.2604>, doi:10.1038/nmeth.2604.

455 Gerber, N.N., 1979. Volatile Substances from Actinomycetes: Their Role in the Odor Pollution of Water. *CRC Critical
456 Reviews in Microbiology* 7, 191–214. doi:10.3109/10408417909082014.

457 Giglio, S., Chou, W.K.W., Ikeda, H., Cane, D.E., Monis, P.T., 2011. Biosynthesis of 2-methylisoborneol
458 in cyanobacteria. *Environmental Science & Technology* 45, 992–998. doi:10.1021/es102992p,
459 arXiv:<http://pubs.acs.org/doi/pdf/10.1021/es102992p>.

460 Halstvedt, C.B., Rohrlack, T., Andersen, T., Skulberg, O., Edvardsen, B., 2007. Seasonal dynamics and depth distribution
461 of *Planktothrix* spp. in Lake Steinsfjorden (Norway) related to environmental factors. *Journal of Plankton Research*
462 29, 471–482. URL: <http://plankt.oxfordjournals.org/content/29/5/471.abstract>, doi:10.1093/plankt/fbm036,
463 arXiv:<http://plankt.oxfordjournals.org/content/29/5/471.full.pdf+html>.

464 Huang, X., Huang, Z., Chen, X.p., Zhang, D., Zhou, J., Wang, X., Gao, N., 2018. The predominant phytoplankton of
465 *Pseudoanabaena* holding specific biosynthesis gene-derived occurrence of 2-MIB in a drinking water reservoir. *En-
466 vironmental Science and Pollution Research* 25, 19134–19142. URL: <https://doi.org/10.1007/s11356-018-2086-z>,
467 doi:10.1007/s11356-018-2086-z.

468 Izaguirre, G., Taylor, W., 2007. Geosmin and MIB events in a new reservoir in southern california. *Water Science &
469 Technology* 55, 9–14.

470 Jia, Z., Su, M., Liu, T., Guo, Q., Wang, Q., Burch, M., Yu, J., Yang, M., 2019. Light as a possible regulator of MIB-producing
471 *Planktothrix* in source water reservoir, mechanism and *in-situ* verification. *Harmful Algae* 88, 101658. URL: <http://www.sciencedirect.com/science/article/pii/S1568988319301313>, doi:10.1016/j.hal.2019.101658.

472

473 Kakimoto, M., Ishikawa, T., Miyagi, A., Saito, K., Miyazaki, M., Asaeda, T., Yamaguchi, M., Uchimiya, H., Kawai-yamada,
474 M., 2014. Culture temperature affects gene expression and metabolic pathways in the 2-methylisoborneol-producing

475 cyanobacterium *Pseudanabaena galeata*. Journal of Plant Physiology 171, 292–300. URL: <http://www.sciencedirect.com/science/article/pii/S017616171300360x>, doi:10.1016/j.jp1ph.2013.09.005.

476

477 Kim, K., Yoon, Y., Cho, H., Hwang, S.J., 2020. Molecular probes to evaluate the synthesis and production potential of

478 an odorous compound (2-methylisoborneol) in cyanobacteria. International Journal of Environmental Research and

479 Public Health 17, 1933. URL: <https://doi.org/10.3390/IJERPH17061933>, doi:10.3390/ijerph17061933.

480 Komarek, J., Kastovsky, J., Mares, J., Johansen, J.R., 2014. Taxonomic classification of cyanoprokaryotes (cyanobacterial

481 genera) 2014, using a polyphasic approach. Preslia 86, 295–335.

482 Komatsu, M., Tsuda, M., Omura, S., Oikawa, H., Ikeda, H., 2008. Identification and functional analysis of genes controlling

483 biosynthesis of 2-methylisoborneol. Proceedings of the National Academy of Sciences 105, 7422–7427. URL: <http://www.pnas.org/content/105/21/7422.abstract>, doi:10.1073/pnas.0802312105.

484

485 Kruskal, J.B., 1964. Nonmetric multidimensional scaling: A numerical method. Psychometrika 29, 115–129. URL: <https://doi.org/10.1007/BF02289694>, doi:10.1007/bf02289694.

486

487 Lanciotti, E., Santini, C., Lupi, E., Burrini, D., 2003. Actinomycetes, cyanobacteria and algae causing tastes and odours in

488 water of the river arno used for the water supply of Florence. Journal of Water Supply: Research and Technology-Aqua

489 52, 489–500. URL: <https://doi.org/10.2166/2Faqua.2003.0044>, doi:10.2166/aqua.2003.0044.

490 Lee, J., Rai, P.K., Jeon, Y.J., Kim, K.H., Kwon, E.E., 2017. The role of algae and cyanobacteria in the production and release

491 of odorants in water. Environmental Pollution 227, 252–262. URL: <http://www.sciencedirect.com/science/article/pii/S0269749117302877>, doi:10.1016/j.envpol.2017.04.058.

492

493 Lee, S., Lee, S., Kim, S.H., Park, H., Park, S., Yum, K., 2012. Examination of critical factors related to summer chlorophyll

494 *a* concentration in the sueo dam reservoir, republic of korea. Environmental Engineering Science 29, 502–510. URL:

495 <https://doi.org/10.1089/2Fees.2011.0070>, doi:10.1089/ees.2011.0070.

496 Li, Z., Hobson, P., An, W., Burch, M.D., House, J., Yang, M., 2012. Earthy odor compounds production and loss in three

497 cyanobacterial cultures. Water Research 46, 5165–5173. URL: <http://www.sciencedirect.com/science/article/pii/S0043135412004046>, doi:10.1016/j.watres.2012.06.008.

498

499 Lu, J., Struewing, I., Wymer, L., Tettenhorst, D.R., Shoemaker, J., Allen, J., 2020. Use of qPCR and RT-qPCR for mon-

500 itoring variations of microcystin producers and as an early warning system to predict toxin production in an Ohio

501 inland lake. Water Research 170, 115262. URL: <https://doi.org/10.1016/2Fj.watres.2019.115262>, doi:10.1016/j.watres.2019.115262.

502

503 Lu, J., Su, M., Su, Y., Wu, B., Cao, T., Fang, J., Yu, J., Zhang, H., Yang, M., 2022. Driving forces for the growth

504 of mib-producing *Planktothricoides raciborskii* in a low-latitude reservoir. Water Research , 118670 URL: <https://www.sciencedirect.com/science/article/pii/S0043135422006236>, doi:10.1016/j.watres.2022.118670.

505

506 Lu, K.Y., Chiu, Y.T., Burch, M., Senoro, D., Lin, T.F., 2019. A molecular-based method to estimate the risk associated with

507 cyanotoxins and odor compounds in drinking water sources. Water Research 164, 114938. URL: <https://doi.org/10.1016/2Fj.watres.2019.114938>, doi:10.1016/j.watres.2019.114938.

508

509 Magoc, T., Salzberg, S.L., 2011. FLASH: fast length adjustment of short reads to improve genome assemblies. Bioinformat-

510 ics 27, 2957–2963. URL: <https://doi.org/10.1093/bioinformatics/btr507>, doi:10.1093/bioinformatics/
511 btr507.

512 Oksanen, J., Blanchet, F.G., Kindt, R., Legendre, P., Minchin, P.R., O'hara, R.B., Simpson, G.L., Solymos, P., Stevens, M.H.H.,
513 Wagner, H., 2014. Vegan: Community Ecology Package. URL: <http://cran.r-project.org/package=vegan>. r Package
514 Version 2.2-0.

515 Persson, P.E., 1996. Cyanobacteria and off-flavours. *Phycologia* 35, 168–171. URL: <https://doi.org/10.2216/i0031-8884-35-6s-168.1>,
516 doi:10.2216/i0031-8884-35-6s-168.1.

517 Qiu, P., Chen, Y., Li, C., Huo, D., Bi, Y., Wang, J., Li, Y., Li, R., Yu, G., 2021. Using molecular detection for the diversity
518 and occurrence of cyanobacteria and 2-methylisoborneol-producing cyanobacteria in an eutrophicated reservoir in
519 Northern China. *Environmental Pollution* 288, 117772. URL: <https://www.sciencedirect.com/science/article/pii/S0269749121013543>,
520 doi:10.1016/j.envpol.2021.117772.

521 R Core Team, 2020. R: A Language and Environment for Statistical Computing. R Foundation for Statistical Computing.
522 Vienna, Austria. URL: <https://www.r-project.org/>.

523 Rangel, L.M., Silva, L.H.S., Rosa, P., Roland, F., Huszar, V.L.M., 2012. Phytoplankton biomass is mainly controlled by
524 hydrology and phosphorus concentrations in tropical hydroelectric reservoirs. *Hydrobiologia* 693, 13–28. URL: <https://doi.org/10.1007/s10750-012-1083-3>,
525 doi:10.1007/s10750-012-1083-3.

526 Rong, C., Liu, D., Li, Y., Yang, K., Han, X., Yu, J., Pan, B., Zhang, J., Yang, M., 2018. Source water odor in one reservoir
527 in hot and humid areas of southern China: occurrence, diagnosis and possible mitigation measures. *Environmental*
528 *Sciences Europe* 30. URL: <https://doi.org/10.1186/s12302-018-0175-8>, doi:10.1186/s12302-018-0175-8.

529 Su, M., An, W., Yu, J., Pan, S., Yang, M., 2014. Importance of underwater light field in selecting phytoplankton morphology
530 in a eutrophic reservoir. *Hydrobiologia* 724, 203–216. URL: <https://doi.org/10.1007/s10750-013-1734-z>, doi:10.
531 1007/s10750-013-1734-z.

532 Su, M., Andersen, T., Burch, M., Jia, Z., An, W., Yu, J., Yang, M., 2019. Succession and interaction of surface and subsurface
533 cyanobacterial blooms in oligotrophic/mesotrophic reservoirs: A case study in Miyun Reservoir. *Science of the Total*
534 *Environment* 649, 1553–1562. URL: <http://www.sciencedirect.com/science/article/pii/S0048969718332789>, doi:10.
535 1016/j.scitotenv.2018.08.307.

536 Su, M., Fang, J., Jia, Z., Su, Y., Zhu, Y., Wu, B., Little, J.C., Yu, J., Yang, M., 2023. Biosynthesis of 2-methylisoborneol is
537 regulated by chromatic acclimation of *Pseudanabaena*. *Environmental Research* , 115260 URL: [https://doi.org/10.](https://doi.org/10.1016/j.envres.2023.115260)
538 [1016/j.envres.2023.115260](https://doi.org/10.1016/j.envres.2023.115260), doi:10.1016/j.envres.2023.115260.

539 Su, M., Yu, J., Zhang, J., Chen, H., An, W., Vogt, R.D., Andersen, T., Jia, D., Wang, J., Yang, M., 2015. MIB-producing
540 cyanobacteria (*Planktothrix* sp.) in a drinking water reservoir: Distribution and odor producing potential. *Water*
541 *Research* 68, 444–453. URL: <http://www.sciencedirect.com/science/article/pii/S004313541400668x>, doi:10.1016/
542 j.watres.2014.09.038.

543 Su, M., Zhu, Y., Jia, Z., Liu, T., Yu, J., Burch, M., Yang, M., 2021. Identification of MIB producers and odor risk assessment
544 using routine data: A case study of an estuary drinking water reservoir. *Water Research* 192, 116848. URL: <http://www.sciencedirect.com/science/article/pii/S0043135421001168>.

545 [//www.sciencedirect.com/science/article/pii/S0043135421000464](https://www.sciencedirect.com/science/article/pii/S0043135421000464), doi:10.1016/j.watres.2021.116848.

546 Sun, D., Yu, J., An, W., Yang, M., Chen, G., Zhang, S., 2013. Identification of causative compounds and microorganisms
547 for musty odor occurrence in the Huangpu River, China. *Journal of Environmental Sciences* 25, 460–465. URL: <http://www.sciencedirect.com/science/article/pii/S1001074212600126>, doi:10.1016/S1001-0742(12)60012-6.

548

549 Suruzzaman, M., Cao, T., Lu, J., Wang, Y., Su, M., Yang, M., 2022. Evaluation of the MIB-producing potential based on
550 real-time qpcr in drinking water reservoirs. *Environmental Research*, 112308 URL: <https://www.sciencedirect.com/science/article/pii/S0013935121016091>, doi:10.1016/j.envres.2021.112308.

551

552 Wang, Z., Li, R., 2015. Effects of light and temperature on the odor production of 2-methylisoborneol-producing *Pseu-*
553 *danabaena* sp. and geosmin-producing *Anabaena ucrainica* (cyanobacteria). *Biochemical Systematics and Ecology*
554 58, 219–226. URL: <http://www.sciencedirect.com/science/article/pii/S0305197814003378>, doi:10.1016/j.bse.
555 2014.12.013.

556 Wang, Z., Xu, Y., Shao, J., Wang, J., Li, R., 2011. Genes associated with 2-methylisoborneol biosynthesis in cyanobacteria:
557 Isolation, characterization, and expression in response to light. *Plos One* 6, E18665. URL: <http://dx.doi.org/10.1371/journal.pone.0018665>, doi:10.1371/journal.pone.0018665.

558

559 Watson, S.B., Monis, P., Baker, P., Giglio, S., 2016. Biochemistry and genetics of taste- and odor-producing cyanobacteria.
560 *Harmful Algae* 54, 112–127. URL: <http://www.sciencedirect.com/science/article/pii/S1568988315301530>, doi:10.
561 1016/j.hal.2015.11.008.

562 Watson, S.B.W.S., Ridal, J.R.J., Boyer, G.L.B.G., 2008. Taste and odour and cyanobacterial toxins: Impair-
563 ment, prediction, and management in the great lakes. *Canadian Journal of Fisheries and Aquatic Sci-*
564 *ences* 65, 1779–1796. URL: <http://www.nrcresearchpress.com/doi/abs/10.1139/f08-084>, doi:10.1139/f08-084,
565 [arXiv:http://www.nrcresearchpress.com/doi/pdf/10.1139/f08-084](http://www.nrcresearchpress.com/doi/pdf/10.1139/f08-084).

566 Wickham, H., 2009. Introduction, in: *ggplot2*. Springer New York, pp. 1–7. URL: http://dx.doi.org/10.1007/978-0-387-98141-3_1, doi:10.1007/978-0-387-98141-3_1.

567

568 Wiltbank, L.B., Kehoe, D.M., 2019. Diverse light responses of cyanobacteria mediated by phytochrome superfamily
569 photoreceptors. *Nature Reviews Microbiology* 17, 37–50. URL: <https://doi.org/10.1038/s41579-018-0110-4>,
570 doi:10.1038/s41579-018-0110-4.

571 Wu, T., Zhu, G., Zhu, M., Xu, H., Yang, J., Zhao, X., 2021. Effects of algae proliferation and density current on the vertical
572 distribution of odor compounds in drinking water reservoirs in summer. *Environmental Pollution* 288, 117683. URL:
573 <https://doi.org/10.1016%2Fj.envpol.2021.117683>, doi:10.1016/j.envpol.2021.117683.

574 Yang, M., Yu, J., Li, Z., Guo, Z., Burch, M., Lin, T.f., 2008. Taihu Lake not to blame for Wuxi's Woes. *Science* 319, 158. URL:
575 <http://www.sciencemag.org/content/319/5860/158.1.short>, doi:10.1126/science.319.5860.158a.

576 Yu, J., Yang, M., fuh Lin, T., Guo, Z., Zhang, Y., Gu, J., Zhang, S., 2007. Effects of surface characteristics of acti-
577 vated carbon on the adsorption of 2-methylisobornel (MIB) and geosmin from natural water. *Separation and Pu-*
578 *riification Technology* 56, 363–370. URL: <http://www.sciencedirect.com/science/article/pii/S1383586607001177>,
579 doi:10.1016/j.seppur.2007.01.039.

580 Zaitlin, B., Watson, S.B., 2006. Actinomycetes in relation to taste and odour in drinking water: Myths, tenets and truths.
581 Water Research 40, 1741–1753. URL: <http://www.sciencedirect.com/science/article/pii/S0043135406001096>,
582 doi:10.1016/j.watres.2006.02.024.

583 Zamyadi, A., Henderson, R., Stuetz, R., Hofmann, R., Ho, L., Newcombe, G., 2015. Fate of geosmin and 2-
584 methylisoborneol in full-scale water treatment plants. Water Research 83, 171–183. URL: <http://www.sciencedirect.com/science/article/pii/S0043135415300889>, doi:10.1016/j.watres.2015.06.038.

585
586 Zhang, T., Zheng, L., Li, L., Song, L., 2016. 2-methylisoborneol production characteristics of *Pseudanabaena* sp. FACHB
587 1277 isolated from xionghe reservoir, China. Journal of Applied Phycology , 1–10URL: <http://dx.doi.org/10.1007/s10811-016-0864-x>, doi:10.1007/s10811-016-0864-x.

588
589 Zimba, P.V., Dionigi, C.P., Millie, D.F., 1999. Evaluating the relationship between photopigment synthesis and 2-
590 methylisoborneol accumulation in cyanobacteria. Journal of Phycology 35, 1422–1429. URL: <http://dx.doi.org/10.1046/j.1529-8817.1999.3561422.x>, doi:10.1046/j.1529-8817.1999.3561422.x.

591
592 Zuo, Y., Li, L., Zhang, T., Zheng, L., Dai, G., Liu, L., Song, L., 2010. Contribution of *Streptomyces* in sediment to earthy odor
593 in the overlying water in xionghe reservoir, China. Water Research 44, 6085–6094. doi:10.1016/j.watres.2010.
594 08.001.